

# Growth Rate-Dependent Regulation of Medial FtsZ Ring Formation

Richard B. Weart and Petra Anne Levin\*

Department of Biology, Washington University, St. Louis, Missouri 63130

Received 22 November 2002/Accepted 11 February 2003

**FtsZ is an essential cell division protein conserved throughout the bacteria and archaea. In response to an unknown cell cycle signal, FtsZ polymerizes into a ring that establishes the future division site. We conducted a series of experiments examining the link between growth rate, medial FtsZ ring formation, and the intracellular concentration of FtsZ in the gram-positive bacterium *Bacillus subtilis*. We found that, although the frequency of cells with FtsZ rings varies as much as threefold in a growth rate-dependent manner, the average intracellular concentration of FtsZ remains constant irrespective of doubling time. Additionally, expressing *ftsZ* solely from a constitutive promoter, thereby eliminating normal transcriptional control, did not alter the growth rate regulation of medial FtsZ ring formation. Finally, our data indicate that overexpressing FtsZ does not dramatically increase the frequency of cells with medial FtsZ rings, suggesting that the mechanisms governing ring formation are refractile to increases in FtsZ concentration. These results support a model in which the timing of FtsZ assembly is governed primarily through cell cycle-dependent changes in FtsZ polymerization kinetics and not simply via oscillations in the intracellular concentration of FtsZ. Importantly, this model can be extended to the gram-negative bacterium *Escherichia coli*. Our data show that, like those in *B. subtilis*, average FtsZ levels in *E. coli* are constant irrespective of doubling time.**

Temporally, cell division must be tightly coupled to chromosome replication, chromosome segregation, and cell growth to ensure that both daughter cells inherit complete genomes and are of the appropriate size and shape. In eukaryotes, the precise orchestration of cyclin-dependent kinases in conjunction with ubiquitin-mediated proteolysis guarantees that each stage of the cell cycle is firmly integrated with the next (22, 28). In bacteria, in which DNA synthesis, chromosome segregation, and cell division can overlap, the factors that govern cell cycle transitions are not clearly defined.

The earliest known event in bacterial cell division is the assembly of the tubulin-like protein FtsZ into a ring structure at the nascent division site in response to an unidentified cell cycle signal (35, 45). FtsZ ring formation has been shown to be required for the recruitment of other division proteins, including components of the cell wall, to the septal site in both *Escherichia coli* and *Bacillus subtilis* (10, 35, 45, 55). Fluorescence microscopy of wild-type and mutant *E. coli* cells indicates that FtsZ first localizes to midcell as a small focus of protein that then extends bidirectionally around the circumference of the cell (2). This observation suggests the presence of a nucleation site that lowers the critical concentration of FtsZ required to initiate polymerization. In response to a second, also unidentified, cell cycle signal the FtsZ ring constricts like a drawstring at the leading edge of the invaginating septum to help mediate cytokinesis (35).

Although the factors responsible for establishing a nucleation site for FtsZ at midcell remain elusive, several proteins are known to prevent aberrant FtsZ ring formation and septation at cell poles in both *E. coli* and *B. subtilis* (49). The MinCD complex is concentrated at cell poles, where, as indi-

cated by biochemical data, it inhibits FtsZ polymerization (21). Genetic and cell biological data suggest that EzrA functions by raising the critical concentration of FtsZ required for assembly, thereby assisting the MinCD complex in preventing ring formation at unfavorable sites like the cell poles (30, 32).

In *B. subtilis*, the frequency of medial FtsZ ring formation varies with growth rate (33). It was previously determined that over 90% of cells growing rapidly in rich medium contained FtsZ rings, whereas only ~60% of cells had FtsZ rings at midcell following growth in a minimal medium (33). This difference in the frequencies of medial FtsZ ring formation presumably reflects differences in the relative numbers of cells that are in the process of dividing under each growth condition and suggests the existence of a cell cycle-dependent mechanism for initiating FtsZ assembly at midcell. Supporting this idea, recent data indicate that medial FtsZ ring formation in both *B. subtilis* and *Caulobacter crescentus* is linked to the initiation of DNA replication (18, 41, 44). In an effort to better understand the regulatory networks responsible for the temporal control of cytokinesis, we have performed a series of experiments examining the growth rate regulation of FtsZ ring formation in *B. subtilis*.

There are several models for the cell cycle-dependent initiation of FtsZ ring formation. For example, FtsZ ring formation is a concentration-dependent phenomenon in both *B. subtilis* and *E. coli*. Lowering the intracellular levels of FtsZ below a critical concentration through the use of an inducible and repressible promoter results first in a block in FtsZ ring formation, followed by filamentation, and eventually cell death (30, 35). Thus, a simple model for the growth rate-dependent regulation of FtsZ ring formation is that FtsZ levels oscillate in a cell cycle-dependent manner, reaching a critical threshold just prior to the initiation of cytokinesis (Fig. 1A). Alternatively, FtsZ levels may remain essentially constant during the cell cycle, and ring formation is governed by a cell cycle-dependent signal that either stimulates the assembly of FtsZ

\* Corresponding author. Mailing address: Department of Biology, Washington University, Campus Box 1137, One Brookings Dr., St. Louis, MO 63130. Phone: (314) 935-7888. Fax: (314) 935-4432. E-mail: plevin@biology.wustl.edu.

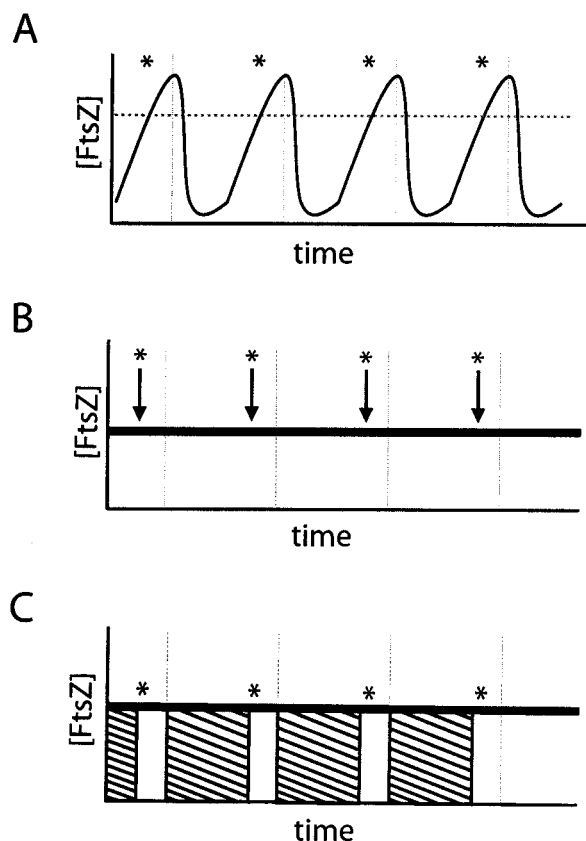


FIG. 1. Alternative models for the regulation of FtsZ ring formation. (A) FtsZ production is regulated in a cell cycle-dependent fashion. As the cell approaches the appropriate time for ring formation (asterisk), intracellular FtsZ levels rise above the critical concentration (horizontal dotted line) for polymerization and allow for the assembly of the FtsZ ring. As the division cycle is completed (vertical lines), FtsZ levels rapidly drop to predivision levels, thereby preventing inappropriate ring formation. (B and C) Alternatively, FtsZ levels remain constant throughout the division cycle. The initiation of ring formation is, instead, controlled by the modulation of FtsZ polymerization dynamics. At the appropriate time, the cell stimulates the assembly of the FtsZ ring from a previously existing pool of monomers by either initiating a positive stimulus of FtsZ polymerization (B, arrows) or by relieving the repression of FtsZ polymerization present during the predivisional period (C, striped boxes).

subunits from a cytoplasmic pool (Fig. 1B) or overrides a division inhibitor that prevents FtsZ assembly at the nascent septal site at the midcell (Fig. 1C).

The role of transcriptional and posttranscriptional regulation of FtsZ in the temporal regulation of bacterial cytokinesis is not clear. In accord with a model in which FtsZ levels oscillate during the course of the bacterial cell cycle (Fig. 1A), *ftsZ* expression has been shown to be subject to growth rate-dependent regulation in *E. coli* (3, 25, 52). In *C. crescentus*, cell cycle-mediated transcriptional regulation and proteolysis are important for maintaining appropriate FtsZ levels (27, 40, 47). However, constitutive expression of *ftsZ* does not induce FtsZ ring formation or constriction in *C. crescentus* swarmer cells that normally do not contain significant levels of FtsZ (42). DNA replication initiation is required for the assembly at the midcell of FtsZ in *C. crescentus* (41), indicating that changes in

the intracellular concentration of FtsZ are not sufficient for the cell cycle-dependent regulation of FtsZ ring formation in this organism.

In *B. subtilis*, the roles of transcriptional regulation and proteolysis in modulating FtsZ ring formation during exponential growth have not been explored. It is known that *ftsZ* transcription is developmentally regulated and that a burst of *ftsZ* expression is important for driving the switch from medial to polar septation at the onset of sporulation (5, 15, 16). Although there is no evidence for or against growth rate-dependent transcriptional regulation, an essential two-component system plays a role in modulating *ftsZ* expression (14). The signal activating this system is not known. However, studies of germinating spores indicate that *ftsZ* transcription is not linked to chromosome replication (18, 46), suggesting that the initiation of FtsZ ring formation does not require a cell cycle-dependent increase in the intracellular concentration of FtsZ.

To begin to clarify the mechanism(s) responsible for the temporal control of FtsZ ring formation, we explored the link between growth rate, the frequency of ring formation, and the intracellular concentration of FtsZ. Our data indicate that fluctuations in FtsZ levels do not play an important role in the growth rate-dependent regulation of FtsZ ring formation in either *B. subtilis* or *E. coli* and therefore support a model in which the assembly of the cytokinetic ring is governed by changes in FtsZ polymerization dynamics during the course of the cell cycle.

#### MATERIALS AND METHODS

**Bacterial strains and plasmids.** All *B. subtilis* strains are derivatives of the strain JH642 (38). Cloning and genetic manipulation were performed by using standard techniques (20, 48). The *E. coli* strain AG1111 (23) was used for cloning, with the exception that the *B. subtilis* *ftsZ* expression vectors were cloned in the AG1111 derivative PL930. PL930 possesses the plasmid pBS58 that overexpresses *E. coli* *ftsZ* and allows for the cloning of *B. subtilis* *ftsZ* in *E. coli* (53).

*E. coli* strain X289 is a wild-type  $F^-$  derivative of strain W1485, a K-12 derivative descended from the original K-12 isolate (9).

*B. subtilis* strain PL950 contains a second copy of *ftsZ*, under the control of the  $P_{spachy}$  promoter (a variant of the  $P_{spac}$  promoter that is 10- to 20-fold stronger than the original  $P_{spac}$  promoter) (32, 43), which is inserted into the chromosome at the *amyE* locus.

*B. subtilis* strain BW121 was constructed by first inserting a second copy of *ftsZ* under the control of the  $P_{xyt}$  promoter into the chromosome at the *thrC* locus. The resulting strain was then transformed with a plasmid carrying a spectinomycin resistance gene (*spc*) flanked upstream by the 3' terminus of *ftsA* and downstream by the 5' terminus of *bpr* to delete the native copy of *ftsZ*. The resulting strain, BW121, is xylose dependent for growth.

**Growth conditions.** (i) *B. subtilis*. For all experiments, overnight cultures of *B. subtilis* strains were diluted with either fresh Luria-Bertani (LB) medium or fresh  $S7_{50}$  minimal medium (24) supplemented with the appropriate amino acids (Trp and Phe, 40  $\mu\text{g}/\text{ml}$ ; Thr, 80  $\mu\text{g}/\text{ml}$ ) and either glucose, glycerol, sorbitol (glucitol), or succinate to a final concentration of 1.0%. Cells were cultured for 3 h at 37°C, at which point they were diluted a second time to an optical density at 600 nm ( $\text{OD}_{600}$ ) of  $\sim 0.025$  in the appropriate media. Cells were then grown to an  $\text{OD}_{600}$  of  $\sim 0.600$  and harvested for analysis via quantitative immunoblotting and immunofluorescence as described below. Samples for the quantitative immunoblotting were washed once with TE buffer (10 mM Tris [pH 8.0], 1 mM EDTA), pelleted, and frozen at  $-80^\circ\text{C}$  for later analysis. Samples for immunofluorescence were prepared as described previously (29).

$P_{xyt}$ -*ftsZ* was induced by the addition of xylose to a final concentration of 0.5%.  $P_{spachy}$ -*ftsZ* was induced, where appropriate, by the addition of IPTG (isopropyl- $\beta$ -D-thiogalactopyranoside) to a final concentration of 10  $\mu\text{M}$  after the second dilution of PL950.

(ii) *E. coli*. Overnight cultures of strain X289, grown in the appropriate media, were diluted to an  $\text{OD}_{600}$  of  $\sim 0.025$  in either fresh LB medium or fresh M9 minimal medium supplemented with either glucose, glycerol, or succinate to a

final concentration of 0.2% (48). Cells were grown to an  $OD_{600}$  of  $\sim 0.250$ . Cells were then harvested for analysis via quantitative immunoblotting as described below. Samples were washed once with TE buffer (10 mM Tris [pH 8.0], 1 mM EDTA), pelleted, and frozen at  $-80^{\circ}\text{C}$  for later analysis.

**Immunofluorescence microscopy.** Immunofluorescence was performed as previously described (29). Briefly, cell samples were prepared by using a paraformaldehyde-glutaraldehyde fixation (2.575% paraformaldehyde and 0.008% glutaraldehyde for cells grown in LB medium and 2.575% paraformaldehyde and 0.0008% glutaraldehyde for cells grown in minimal media). Fixed cells were adhered to the slide with poly-L-lysine and treated with affinity-purified polyclonal rabbit anti-FtsZ antibody (31) and donkey anti-rabbit antibody conjugated to the fluorophore Cy-3 (Molecular Probes, Eugene, Oreg.). Nucleoids were visualized by treatment with the DNA fluorescent stain DAPI. Images were captured by using either an Olympus BX51 microscope with a black and white charge-coupled device OrcaERG camera (Hamamatsu Photonics, Bridgewater, N.J.) in conjunction with the Openlabs version 3.0.9 software (Improvision, Lexington, Mass.) or a Zeiss Axioskop 2 with an Axiocam camera in conjunction with the Axiovision software version 2.05 (Carl Zeiss MicroImaging, Thornwood, N.Y.). Images were processed with Adobe Photoshop version 6.0.1 (Adobe Systems, Mountain View, Calif.).

**Quantitative immunoblotting.** *B. subtilis* cell samples were washed with TE buffer (10 mM Tris [pH 8.0], 1 mM EDTA) and resuspended in lysis buffer (50 mM Tris [pH 8.0], 1 mM EDTA, 100 mM NaCl). Cells were sonicated, and cell lysates were centrifuged at  $16,000 \times g$  to remove cellular debris. The total protein concentration of the cell lysates was then determined by the bicinchoninic acid assay (Pierce Chemical Company, Rockford, Ill.). Cell lysates were normalized to the total protein concentration at gel loading and subjected to sodium dodecyl sulfate-polyacrylamide gel electrophoresis. To ensure that our results were not affected by our preparation method, we performed duplicate experiments in which cells were lysed with lysozyme and detergent and loading was normalized to the  $OD_{600}$  at sampling. Immunoblot analysis was performed by using affinity-purified polyclonal rabbit anti-FtsZ antibodies (31) and goat anti-rabbit antibodies conjugated to horseradish peroxidase (Jackson ImmunoResearch Laboratories, West Grove, Pa.) (17). Immunoblots were developed by using the ChemiDetect kit (Bio-Rad) and visualized and quantified with the luminescent image analyzer LAS-1000plus in conjunction with ImageGauge software version 3.41 (Fuji Film Company, Ltd.). The linear range for the signal was established by serial dilutions of whole-cell lysates and purified FtsZ protein. Based on dilution ratios, we determined that a twofold change in signal intensity corresponded directly to a twofold change in protein levels.

*E. coli* cell samples were either resuspended in Laemmli sample buffer and lysed by repeated freezing and thawing or resuspended in lysis buffer (50 mM Tris [pH 8.0], 1 mM EDTA, 100 mM NaCl) and sonicated. Depending on the method used to break the cells, lysates were normalized to the  $OD_{600}$  or the total protein concentration at gel loading and subjected to sodium dodecyl sulfate-polyacrylamide gel electrophoresis. Immunoblot analysis was performed by using polyclonal rabbit anti-*E. coli* FtsZ antibody, the gift of Joe Lutkenhaus, and goat anti-rabbit antibodies conjugated to horseradish peroxidase (Jackson ImmunoResearch Laboratories) (17). Immunoblots were developed as described above.

**Statistical analysis.** Margins of error for both *B. subtilis* and *E. coli* samples were calculated following quantification of FtsZ immunoblots from three independent experiments (i.e., three separate sets of cultures). Confidence intervals were generated by using a *t* test with a 95% confidence level.

## RESULTS

**The frequency of FtsZ ring formation varies with growth rate in *B. subtilis*.** It was previously determined that the frequency of medial FtsZ ring formation in exponentially growing *B. subtilis* cells varies as a function of mass doubling time (33). To extend these observations, we examined the frequency of cells with FtsZ rings at midcell after growth in four different media: LB medium, minimal glucose, minimal sorbitol, and minimal succinate.

Wild-type *B. subtilis* cells (JH642) were cultured in each medium until mid-exponential growth phase ( $OD_{600} = 0.6$ ), at which point samples were removed and processed for immunofluorescence microscopy and quantitative immunoblotting. Mass doubling times in the four different media ranged from

26 min in LB medium to 94 min in minimal succinate at  $37^{\circ}\text{C}$ . We scored cells as positive for FtsZ ring formation if they possessed two spots of fluorescence adjacent to one another at the midcell, a band of fluorescence across midcell, or a medial point of fluorescence (representing a constricting FtsZ ring). Although we occasionally observed polar FtsZ rings ( $<0.6\%$  in LB medium), only those cells with medial FtsZ rings were scored as positive.

Cells grown in rich medium with a rapid doubling time had a significantly higher frequency of FtsZ rings than those grown in minimal medium with a slow doubling time (Fig. 2 and 3). As shown in Fig. 2A to C, 85.3% (1,366 of 1,601) of cells cultured in LB medium (doubling time, 26 min) had FtsZ rings. In contrast (Fig. 2D to F), only 33.9% (449 of 1,326) of cells grown in minimal succinate (doubling time, 94 min) had medial rings. This result is consistent with previous observations (31, 33).

Our data suggest that rapidly growing cells must initiate FtsZ ring formation and thus cell division soon after the end of the previous cell cycle. By contrast, slow-growing cells exhibit a significant delay (approximately 60 min in minimal succinate) between the end of the previous cell cycle and the assembly of the division apparatus. Our results are thus consistent with those of Boye et al. and Den Blaauwen et al. (6, 11) which indicate that under slow growth conditions the *E. coli* cell cycle begins to resemble that of eukaryotic cells in which cell division is followed by a growth period or gap ( $G_1$ ), DNA synthesis (S), a second gap ( $G_2$ ), and finally the next cell division.

**The average intracellular concentration of FtsZ in *B. subtilis* is constant regardless of growth rate.** FtsZ ring formation requires the presence of a threshold concentration of FtsZ (30, 35), and thus a simple explanation for the differences that we observed in the frequencies of rings under the four growth conditions is that FtsZ assembly is modulated by cell cycle-dependent oscillations in FtsZ levels (Fig. 1A). If this model is correct, we would expect FtsZ concentration, as a proportion of total protein, to be high in a population of rapidly growing cells and low in a population of slow-growing cells, reflecting the differences in the frequencies of FtsZ ring formation.

To measure FtsZ levels, we sampled *B. subtilis* cells after growth in the four different media described above. Following sonication and removal of insoluble material by centrifugation, cell lysates were normalized for total protein concentration and separated on a polyacrylamide gel. Relative FtsZ levels were determined by quantitative immunoblotting in conjunction with band intensity analysis performed by using the LAS-1000plus luminescent image analyzer (Fuji) and ImageGauge software version 3.41. To validate the efficacy of our approach, we also lysed cells by using lysozyme and detergent and normalized lysates to equivalent cell mass based on the  $OD_{600}$  prior to lysis. We obtained identical results regardless of the method (data not shown). Finally, as additional controls, the linear range for the signal was established by serial dilutions of whole-cell lysates and purified FtsZ protein. Within the linear range for the chemiluminescent signal, we determined that a twofold change in signal intensity corresponded directly with a twofold change in protein levels.

FtsZ levels remained essentially constant under all of the growth conditions that we examined (Fig. 4). This result indicates that the average intracellular concentration of FtsZ re-

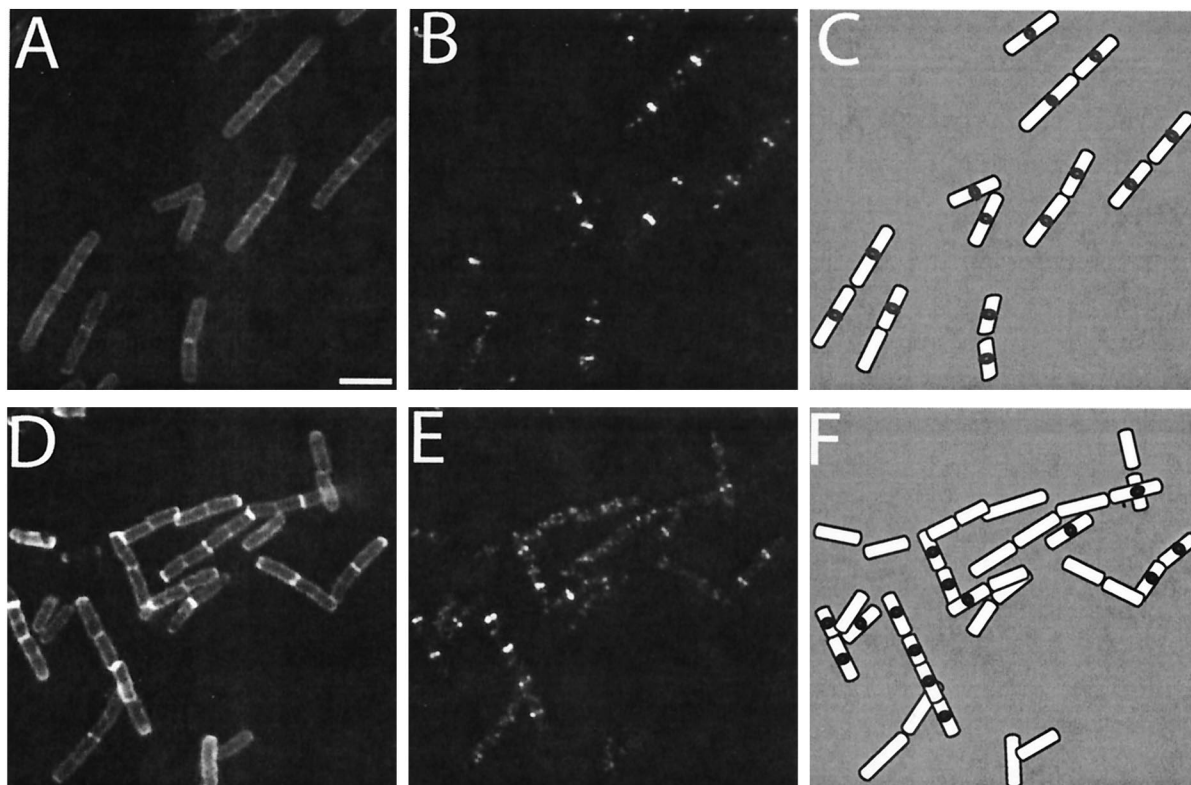


FIG. 2. The frequency of FtsZ ring formation varies with growth rate in *B. subtilis*. Wild-type cells were grown in either LB medium (A to C) or minimal succinate (D to F). (A and D) Cell walls stained with wheat germ agglutinin conjugated to fluorescein isothiocyanate. (B and E) FtsZ immunolocalized by using affinity-purified primary antibody and secondary antibody conjugated to Cy-3. (C and F) Drawings of merged images. Scale bar, 2  $\mu$ m.

mains constant regardless of doubling time. As an internal control, we also measured RecA levels by using antisera against *B. subtilis* RecA, the generous gift of Charles Lovett. Like those of FtsZ, levels of RecA were constant regardless of growth rate (data not shown).

**The frequency of FtsZ ring formation is growth rate dependent in *B. subtilis* even when *ftsZ* is expressed constitutively.** To determine what contribution native transcriptional regulation plays in the control of FtsZ assembly in *B. subtilis*, we examined FtsZ ring formation and FtsZ levels in cells in which *ftsZ* was expressed from a constitutive promoter. For these experiments, we initially employed  $P_{spac}$ , an IPTG-inducible, LacI-repressible promoter commonly used for gene expression studies with *B. subtilis* (58), to drive *ftsZ* expression. However, we found that this promoter is subject to strong growth rate-dependent regulation. While  $P_{spac}$  expression was robust in LB medium, expression decreased dramatically with increasing doubling times (data not shown). As  $P_{spac}$  is a hybrid promoter derived from the bacteriophage *spo1* promoter (58), this growth rate regulation may reflect some unexplored aspect of bacteriophage biology. For these experiments, we therefore took advantage of a strain (BW121) engineered to express *ftsZ* at the threonine locus from a xylose-inducible, XylR-repressible promoter ( $P_{xyl}$ ) (4). In our study, expression from  $P_{xyl}$  was constant regardless of growth rate (data not shown). The native allele of *ftsZ* has been disrupted in BW121. Thus, all *ftsZ* is transcribed from  $P_{xyl}$ , rendering the strain xylose dependent

for growth and viability. This strain also carries a tetracycline drug resistance cassette (*tet*) inserted into *xylA*, encoding xylose isomerase (4), to preclude it from using xylose as a carbon source.

Employing this strain, we measured doubling times, medial FtsZ ring frequencies, and FtsZ levels after growth in LB medium, minimal glycerol, minimal sorbitol, and minimal succinate supplemented with 0.5% xylose. (We selected minimal glycerol instead of minimal glucose for these experiments to avoid complications from catabolite repression of  $P_{xyl}$ .) The doubling times of the  $P_{xyl}$ -*ftsZ* strain did not differ significantly from those of wild-type cells under equivalent growth conditions (Fig. 3). Moreover, when fully induced (0.5% xylose), FtsZ levels in our engineered cells were constant under all growth conditions and approximately equivalent to those in wild-type cells (data not shown).

As in wild-type cells, we found that the frequency of FtsZ ring formation in our engineered strain was growth rate dependent. In LB medium, with a doubling time of 23 min, the  $P_{xyl}$ -*ftsZ* strain had a frequency of FtsZ ring formation of 85.6% (421 of 492). By contrast, the frequency of ring formation in the same strain fell to only 29.9% (159 of 531) after growth in minimal succinate (doubling time, 99 min.) These data are similar to those obtained for wild-type cells and, significantly, describe the same linear curve with regard to FtsZ ring frequency and doubling time (Fig. 3). These results indicate that growth rate, and not transcription-dependent

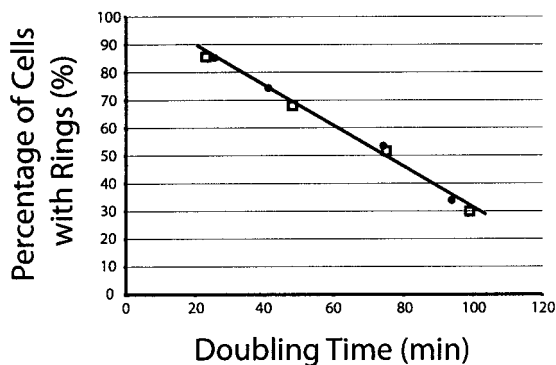


FIG. 3. Plot of the frequencies of cells with medial FtsZ rings versus doubling times. Wild-type *B. subtilis* cells (JH642; filled circles) were grown in LB medium, minimal glucose, minimal sorbitol, and minimal succinate to produce doubling times of 26, 41, 74, and 94 min, respectively. The FtsZ ring frequencies for these cultures were 85% (1,366 of 1,601) for LB medium, 75% (828 of 1,104) for minimal glucose, 53% (698 of 1,305) for minimal sorbitol, and 34% (449 of 1,326) for minimal succinate. A *B. subtilis* strain expressing *ftsZ* solely from a xylose-inducible promoter (BW121; unfilled squares) was grown in LB medium, minimal glycerol, minimal sorbitol, and minimal succinate to produce doubling times of 23, 48, 75, and 99 min, respectively. The FtsZ ring frequencies for these cultures were 86% (421 of 492) for LB medium, 68% (349 of 513) for minimal glycerol, 52% (263 of 509) for minimal sorbitol, and 30% (159 of 531) for minimal succinate.

variations in the intracellular concentration of FtsZ, is the primary determinant governing the frequency of medial FtsZ ring formation.

**A twofold increase in FtsZ levels does not override growth rate-dependent control of FtsZ ring formation in *B. subtilis*.** Although our data indicate that FtsZ concentrations remain essentially constant over a range of growth rates (Fig. 4), it is possible that small, cell cycle-regulated changes in FtsZ levels, undetectable by immunoblotting, may be controlling ring formation (e.g., FtsZ levels are maintained just below a critical threshold and ring formation is initiated by a slight increase [ $<10\%$ ] in the intracellular concentration of FtsZ at the appropriate point in the cell cycle). To test this possibility and determine if it is possible to override the growth rate-dependent regulation of ring formation in *B. subtilis* by increasing FtsZ levels, we constructed a strain in which a second copy of *ftsZ* was placed under the control of a modified version of the LacI-repressible, IPTG-inducible promoter *P<sub>spac</sub>* (43) at the amylase locus (PL950). This promoter (*P<sub>spachy</sub>*) is 10- to 20-fold stronger than *P<sub>spac</sub>* (43).

Using this *P<sub>spachy</sub>-ftsZ*-bearing strain, we selected an intermediate growth condition, minimal sorbitol, and titrated IPTG concentration to achieve a modest increase in FtsZ levels. As shown (Fig. 5A), the intracellular concentration of FtsZ in these cells was approximately equivalent to that in wild-type cells in the absence of IPTG. The addition of IPTG to a concentration of 10  $\mu$ M, however, boosted FtsZ levels more than twofold in the *P<sub>spachy</sub>-ftsZ* strain.

It has been previously determined that overexpressing FtsZ to similar levels in *B. subtilis* cells growing in LB medium leads to the formation of extra FtsZ rings at polar positions (32). Similarly, overexpressing FtsZ two- to sevenfold in *E. coli* leads to the formation of polar septa and minicells (54). These data were interpreted to indicate that increases in FtsZ concentra-

tions stabilized the FtsZ polymer such that it was able to overcome the inhibitory actions of the MinCD complex at cell poles (32). Consistent with previous observations, we found that a twofold increase in FtsZ levels in *B. subtilis* cells growing in minimal sorbitol doubled the frequency of polar FtsZ rings. In the absence of IPTG, 2.5% (30 of 1,180) of PL950 cells bearing *P<sub>spachy</sub>-ftsZ* had at least one polar FtsZ ring under these growth conditions (we consistently find that the frequency of cells with polar rings increases to a limited degree with decreasing growth rate, although the reason for this phenomenon is not clear). Several hours after the induction of *P<sub>spachy</sub>-ftsZ*, the frequency of PL950 cells with polar rings rose to 4.7% (74 of 1,552) (2.9% [31 of 1,071] of wild-type cells had at least one polar FtsZ ring after growth in minimal sorbitol).

Although the frequency of cells displaying polar FtsZ rings increased only twofold, we observed a 10-fold increase in the number of cells with double rings at midcell after the induction of *P<sub>spachy</sub>-ftsZ* (Fig. 5B). Among *P<sub>spachy</sub>-ftsZ*-bearing cells, 3.6% (32 of 1,552) had two FtsZ rings adjacent to one another at the midcell in the presence of IPTG. By contrast, in the absence of IPTG, only 0.3% (3 of 1,180) of these cells and 0.2% (2 of

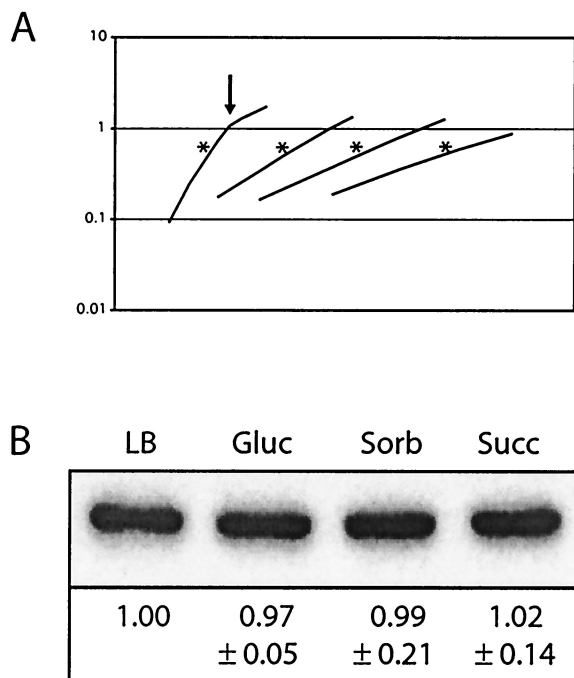


FIG. 4. FtsZ levels remain constant regardless of growth rate. (A) Representative growth curves for wild-type *B. subtilis* cells grown in LB medium, minimal glucose (Gluc), minimal sorbitol (Sorb), or minimal succinate (Succ) (from left to right, respectively). Samples were harvested at an  $OD_{600}$  of  $\sim 0.600$ , which is marked in the figure by an asterisk. Arrows, when present, indicate where a culture has exited from exponential-phase growth.  $OD_{600}$  is shown on the y axis. (B) Representative quantitative immunoblot of FtsZ from wild-type *B. subtilis* cells grown in LB medium, minimal glucose, minimal sorbitol, and minimal succinate. Samples were harvested during exponential growth and normalized to total protein at gel loading. Relative concentrations of FtsZ, normalized to those for wild-type cells grown in LB medium, are shown below. Margins of error were calculated by using a *t* test with a 95% confidence level and are based on data from three independent experiments (i.e., three separate sets of cultures).

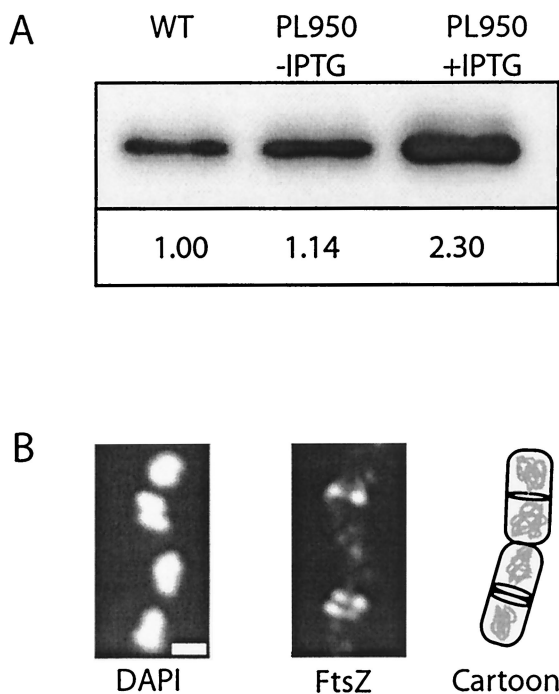


FIG. 5. Overexpression of FtsZ following induction of *P<sub>spachy</sub>-ftsZ*. (A) Quantitative immunoblot of FtsZ from wild-type (WT) cells (left) and PL950 cells bearing *P<sub>spachy</sub>-ftsZ* in the absence (middle) and presence (right) of 10 M IPTG. Samples were harvested during mid-exponential growth, and lysates were normalized to total protein concentration at gel loading. Relative concentrations of FtsZ, normalized to those for the wild type, are shown below. (B) FtsZ localization in cells overexpressing FtsZ. (Left) DNA. (Middle) FtsZ. (Right) Cartoon depicting the position of the FtsZ rings relative to the nucleoids. Note the doublet of FtsZ in the lower cell. Scale bar, 0.5  $\mu$ m.

1,071) of wild-type cells had double rings. In all cases, the double rings flanked the cells' midlines and were the same distance from the most proximal pole. The presence of these double medial rings suggests that at least under certain growth conditions, the medial site can support the formation of more than one FtsZ ring. Multiple rings of FtsZ at midcell have also been observed in *C. crescentus* following FtsZ overexpression, suggesting that this might be a general phenomenon (42). Alternatively, a boost in FtsZ levels in *B. subtilis* at the onset of sporulation and overexpression of FtsZ in *E. coli* have both been shown to generate spiral filaments of FtsZ that extend the length of the cell (5, 36). It is, therefore, possible that the double medial rings we observed following FtsZ overexpression in exponentially growing *B. subtilis* were in fact a single spiral that cannot be resolved by traditional fluorescence microscopy.

If medial FtsZ ring formation is primarily a concentration-dependent phenomenon (Fig. 1A), increasing the intracellular concentration of FtsZ should induce FtsZ assembly at midcell earlier in the cell cycle and, thus, result in an increase in the frequency of cells with medial FtsZ rings. In other words, if small changes in the intracellular concentration of FtsZ are sufficient to account for the growth rate-dependent regulation of medial ring formation, raising FtsZ levels twofold should increase the frequency of cells with FtsZ rings at midcell to a

similar degree (i.e., if 50% of cells normally have medial rings following growth in minimal sorbitol, we would expect that more than 95% of these cells would have FtsZ rings at midcell following a twofold increase in the intracellular concentration of FtsZ). Counter to a concentration-dependent model for FtsZ assembly at midcell (Fig. 1A), we found that a twofold increase in the intracellular concentration of FtsZ (Fig. 5) resulted in only a small increase in the frequency of cells with medial FtsZ rings. In the absence of inducer, 55.5% (655 of 1,180) of cells bearing *P<sub>spachy</sub>-ftsZ* had at least one FtsZ ring at midcell. Following the addition of IPTG, the frequency of cells with medial FtsZ rings increased to only 61.2% (951 of 1,552). Thus, although the number of cells with FtsZ rings is elevated following the induction of *P<sub>spachy</sub>-ftsZ*, the increase in the frequency of medial FtsZ ring formation (5.7%) is not consistent with the increase that would be predicted if a primarily concentration-dependent mechanism were driving FtsZ assembly.

We routinely observe a subset of cells with faint rings of FtsZ in strains expressing an *ftsZ-gfp* fusion (R. B. Weart and P. A. Levin, unpublished data). Thus, it is likely that the small increase we observed in the frequency of cells with medial rings following the induction of *P<sub>spachy</sub>-ftsZ* is primarily the result of increases in the intracellular concentration of FtsZ that render the ring more visible by immunofluorescence microscopy. In addition, cell length measurements suggest that cells in which FtsZ is overexpressed may undergo medial division before they have reached full size and/or have a relatively high frequency of polar division that results in a reduction in average cell size. We determined that cells bearing *P<sub>spachy</sub>-ftsZ* are approximately 10% shorter when FtsZ is overexpressed twofold in the presence of 10  $\mu$ M IPTG than they are in the absence of an inducer. This observation is similar to data for *E. coli* indicating that overexpression of FtsZ in this organism increases the frequency of cytokinesis at midcell as well as at cell poles (54).

**Average FtsZ levels in *E. coli* are constant regardless of growth rate.** As it does in *B. subtilis*, the frequency of FtsZ ring formation varies with growth rate in *E. coli* (11). Our result demonstrating that FtsZ levels remain constant in *B. subtilis* regardless of growth rate, however, contrasts with previous data for *E. coli* indicating that *ftsZ* transcription rates and protein levels decrease with increasing growth rates; i.e., *ftsZ* transcription is higher in cells grown in minimal medium than in cells grown in LB medium (3, 52). We measured FtsZ concentrations in *E. coli* cells cultured under different growth conditions. Again, multiple methods of sample preparation were carried out. Aldea et al. previously performed immunoblotting on *E. coli* cells grown in LB medium, minimal glucose, and minimal glycerol. They concluded that the average intracellular concentration of FtsZ is approximately threefold lower in LB medium than in minimal glycerol (3). We quantified FtsZ levels in the *E. coli* strain X289, a K-12 derivative (the gift of R. Curtiss III), after growth in LB medium or M9 minimal medium supplemented with glucose, glycerol, or succinate. The doubling time for X289 was 24.4 min in LB medium, 63.8 min in M9 glucose, 80.6 min in M9 glycerol, and 119.7 min in M9 succinate. Our results indicate that there is no significant difference in the average intracellular concentrations of FtsZ between *E. coli* cells grown in LB medium and those grown in minimal glucose, minimal glycerol, or minimal succinate when cells are sampled during early ( $OD_{600} = 0.25$ ) exponential

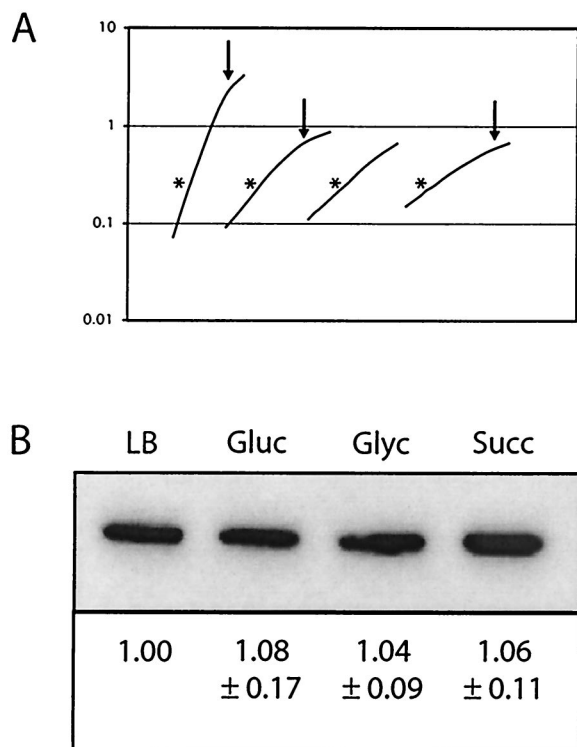


FIG. 6. FtsZ levels in *E. coli* remain constant regardless of growth rate. (A) Representative growth curves for wild-type *E. coli* cells grown in LB medium, minimal glucose, minimal glycerol, and minimal succinate (from left to right, respectively). Samples were harvested at an  $OD_{600}$  of  $\sim 0.250$ , which is marked by an asterisk. Arrows, when present, indicate where a culture has exited from exponential-phase growth.  $OD_{600}$  is shown on the y axis. (B) Representative quantitative immunoblot of FtsZ from wild-type *E. coli* cells grown in LB medium, minimal glucose, minimal glycerol, and minimal succinate. Samples were harvested during exponential growth and normalized to an  $OD_{600}$  of  $\sim 0.250$  at gel loading. Relative concentrations of FtsZ, normalized to those for wild-type cells grown in LB medium, are shown below. Margins of error were calculated by using a *t* test with a 95% confidence level and are based on data from three independent experiments (i.e., three separate sets of cultures).

phase (Fig. 6). This is true whether samples are normalized to the  $OD_{600}$ , as was done in the original *E. coli* experiments (Fig. 6) (3), or to total protein (data not shown).

Although it is unclear why our data differ from those of Aldea et al., we consistently observe that FtsZ levels do not vary with growth rate in either *B. subtilis* or *E. coli*. Thus, our data support the idea that changes in polymerization kinetics, rather than oscillations in the intracellular concentrations of FtsZ, govern the growth rate regulation of FtsZ ring formation and cytokinesis in *E. coli* as well as in *B. subtilis*.

## DISCUSSION

Consistent with our previous observations as well as with results of studies of exponentially growing *E. coli* (11, 33), we find that the frequency of *B. subtilis* cells with FtsZ rings varies as much as threefold with growth rate (Fig. 2 and 3), presumably reflecting differences in the frequencies of cytokinesis under each growth condition. Quantitative immunoblotting of

cells grown in four different media indicates that average FtsZ levels remain constant despite an almost threefold change in the frequency of cells with FtsZ rings (Fig. 4B). Thus, our data support a model in which FtsZ assembly is driven not by changes in the intracellular concentration of FtsZ (Fig. 1A), but rather by cell cycle signals that either stimulate polymerization of FtsZ subunits from a cytoplasmic pool (Fig. 1B) or release FtsZ from an inhibitor, allowing it to assemble at midcell (Fig. 1C).

In an extension of these experiments and in contrast to previous data from another laboratory (3), we determined that FtsZ levels remain constant in *E. coli* cells regardless of growth rate (Fig. 6). FtsZ levels are also similar in mixed populations of *C. crescentus* cells grown in rich medium (PYE) and minimal medium (M2G) (42). Together, these results suggest that the growth rate-dependent regulation of FtsZ transcription or protein stability is unlikely to be a general mechanism for the temporal regulation of FtsZ assembly and division in bacteria.

**A checkpoint governing FtsZ assembly at midcell?** The growth rate-dependent regulation of FtsZ assembly appears to be extremely robust. Cells expressing *ftsZ* from a  $P_{337}$  promoter exhibit a frequency of FtsZ ring formation that is essentially identical to that observed in wild-type cells (Fig. 3). Moreover, *B. subtilis* cells are refractile to increases in the intracellular concentration of FtsZ with regard to the timing of medial FtsZ ring formation. We found that although overexpression of FtsZ doubled the frequency of polar FtsZ rings, it was not sufficient to override the mechanisms controlling the temporal regulation of medial FtsZ ring formation. Together these data indicate that medial FtsZ ring formation in *B. subtilis* requires more than threshold levels of FtsZ and support the existence of a checkpoint that prevents FtsZ assembly at midcell until the appropriate cell cycle signal has been received.

There are several, not necessarily mutually exclusive, models to account for the temporal regulation of medial FtsZ ring formation: (i) FtsZ is unable to assemble at midcell early in the cell cycle due to the absence of an available nucleation site at this position; (ii) the FtsZ nucleation site is present at midcell for most, if not all, of the cell cycle, but an inhibitor or set of inhibitors prevent FtsZ assembly until the appropriate cell cycle signal has been received; and (iii) the physical presence of the unsegregated nucleoid (nucleoid occlusion) prevents FtsZ assembly at midcell early in the cell cycle, as has been suggested for *E. coli* (37).

In light of our finding that overexpression of FtsZ did not override the growth rate-dependent regulation of medial ring formation, we favor the first model, that FtsZ assembly at midcell is coupled to the formation of a nucleation site at this location. This model is further supported by data for germinating spores indicating that the formation of a medial nucleation site is linked to the initiation of DNA replication (18, 44). Similarly, medial FtsZ ring formation in *C. crescentus* requires the initiation of DNA replication, a cell cycle event that presumably takes place only upon differentiation of swarmer cells into reproductively competent stalked cells (41).

Nucleoid occlusion presents an attractive model for both the spatial and temporal regulation of FtsZ assembly, and there is clear evidence that the nucleoid can act as an inhibitor of FtsZ assembly. FtsZ rings do not form in exponentially growing wild-type cells until chromosome replication is nearly complete

and the nucleoids have separated from one another (11, 18, 37, 44). In addition, when DNA replication or partitioning is blocked, FtsZ rings form adjacent to, not over, the medially positioned nucleoid (19, 50, 51). There is extensive evidence for *B. subtilis*, however, that the nucleoid is not sufficient to prevent FtsZ ring formation and septation (7, 8, 56, 57). Thus, while it may play a role in delaying FtsZ assembly at midcell, nucleoid occlusion is unlikely to be the primary determinant of medial FtsZ ring formation in *B. subtilis*. Ultimately, a comprehensive understanding will require that we both determine the precise nature of the cell cycle signal(s) responsible for initiating FtsZ assembly and identify the factor(s) that establishes the FtsZ nucleation site at midcell.

**A system poised for assembly.** It is becoming apparent that FtsZ ring formation is governed by mechanisms similar in function if not in form to those controlling microtubule formation during the eukaryotic cell cycle. In both cases, it appears that a precisely balanced regulatory network of positively and negatively acting factors modulates polymerization dynamics to ensure that FtsZ ring formation and microtubule assembly occur at the appropriate time and at the correct location (1, 12, 32, 39). As we observed with FtsZ, *Saccharomyces cerevisiae* cells with extra copies of *TUB1* and *TUB2* (which encode  $\alpha$  and  $\beta$  tubulin, respectively) are phenotypically normal despite a modest increase in the intracellular concentration of the tubulin heterodimer (26). These data suggest that eukaryotic cells may also be buffered in some way against changes in the concentration of essential cytoskeletal proteins.

Recent estimates indicate that there are ~5,000 FtsZ molecules in each *B. subtilis* cell grown in CH (hydrolyzed casein) medium (13). Similarly, there are estimated to be approximately 15,000 molecules of FtsZ per *E. coli* cell during exponential growth in LB medium (34). Based on these data and volume estimates for *E. coli* cells, FtsZ levels in both *B. subtilis* and *E. coli* should be well above the minimal concentration required to initiate polymerization in vitro (34). Together with our results, these data suggest that precise transcriptional and/or posttranscriptional regulation of FtsZ is largely dispensable for modulating the timing of FtsZ ring formation. Instead, they support a scenario in which FtsZ is poised to assemble in response to a signal from the cell cycle machinery, rendering cytokinetic ring formation exquisitely sensitive to changes in growth rate.

#### ACKNOWLEDGMENTS

We thank members of the Levin lab for useful discussions during the course of this research. We also thank the Amend lab for the use of their microscope, the Kranz lab for access to the LAS-1000plus luminescent image analyzer, Roy Curtiss for the gift of *E. coli* strain X289, and Charles Lovett and Joseph Lutkenhaus for antisera. We are indebted to Frank Solomon, Sigal Ben-Yehuda, Robert Kranz, Richard Losick, Susan Rowland, Ellen Quardokus, and Marla Chesnik for insightful comments on the manuscript.

This work was supported, in part, by Public Health Services grant GM64671 from the NIH.

#### REFERENCES

1. Addinall, S. G., and B. Holland. 2002. The tubulin ancestor, FtsZ, draughtsman, designer and driving force for bacterial cytokinesis. *J. Mol. Biol.* **318**: 219–236.
2. Addinall, S. G., and J. Lutkenhaus. 1996. FtsZ-spirals and -arcs determine the shape of the invaginating septa in some mutants of *Escherichia coli*. *Mol. Microbiol.* **22**:231–237.
3. Aldea, M., T. Garrido, J. Pla, and M. Vicente. 1990. Division genes in *Escherichia coli* are expressed coordinately to cell septum requirements by gearbox promoters. *EMBO J.* **9**:3787–3794.
4. Arigoni, F., K. Pogliano, C. D. Webb, P. Stragier, and R. Losick. 1995. Localization of protein implicated in establishment of cell type to sites of asymmetric division. *Science* **270**:637–640.
5. Ben-Yehuda, S., and R. Losick. 2002. Asymmetric cell division in *B. subtilis* involves a spiral-like intermediate of the cytokinetic protein FtsZ. *Cell* **109**: 257–266.
6. Boye, E., T. Stokke, N. Kleckner, and K. Skarstad. 1996. Coordinating DNA replication initiation with cell growth: differential roles for DnaA and SeqA proteins. *Proc. Natl. Acad. Sci. USA* **93**:12206–12211.
7. Britton, R. A., and A. D. Grossman. 1999. Synthetic lethal phenotypes caused by mutations affecting chromosome partitioning in *Bacillus subtilis*. *J. Bacteriol.* **181**:5860–5864.
8. Britton, R. A., D. C.-H. Lin, and A. D. Grossman. 1998. Characterization of a prokaryotic SMC protein involved in chromosome partitioning. *Genes Dev.* **12**:1254–1259.
9. Curtiss, R., III, L. J. Charamella, C. M. Berg, and P. E. Harris. 1965. Kinetic and genetic analyses of D-cycloserine inhibition and resistance in *Escherichia coli*. *J. Bacteriol.* **90**:1238–1250.
10. Daniel, R. A., E. J. Harry, V. L. Katis, R. G. Wake, and J. Errington. 1998. Characterization of the essential cell division gene *ftsL* (*ylld*) of *Bacillus subtilis* and its role in the assembly of the division apparatus. *Mol. Microbiol.* **29**:593–604.
11. Den Blaauwen, T., N. Buddelmeijer, M. E. Aarsman, C. M. Hameete, and N. Nanninga. 1999. Timing of FtsZ assembly in *Escherichia coli*. *J. Bacteriol.* **181**:5167–5175.
12. Desai, A., and T. J. Mitchison. 1997. Microtubule polymerization dynamics. *Annu. Rev. Cell Dev. Biol.* **13**:83–117.
13. Feucht, A., I. Lucet, M. D. Yudkin, and J. Errington. 2001. Cytological and biochemical characterization of the FtsA cell division protein of *Bacillus subtilis*. *Mol. Microbiol.* **40**:115–125.
14. Fukuchi, K., Y. Kasahara, K. Asai, K. Kobayashi, S. Moriya, and N. Ogasawara. 2000. The essential two-component regulatory system encoded by *ycfF* and *ycfG* modulates expression of the *ftsAZ* operon in *Bacillus subtilis*. *Microbiology* **146**:1573–1583.
15. Gholamhoseinian, A., Z. Shen, and P. Piggot. 1992. Regulation of the cell division gene *ftsA* during sporulation of *Bacillus subtilis*. *J. Bacteriol.* **174**: 4647–4656.
16. Gonzy-Tréboul, G., C. Karamzyn-Campelli, and P. Stragier. 1992. Developmental regulation of transcription of the *Bacillus subtilis* *ftsAZ* operon. *J. Mol. Biol.* **224**:967–979.
17. Harlow, E., and D. Lane. 1988. *Antibodies: a laboratory manual*. Cold Spring Harbor Laboratory, Cold Spring Harbor, N.Y.
18. Harry, E. J. 2001. Bacterial cell division: regulating Z-ring formation. *Mol. Microbiol.* **40**:795–803.
19. Harry, E. J., J. Rodwell, and R. G. Wake. 1999. Co-ordinating DNA replication with cell division in bacteria: a link between the early stages of a round of replication and mid-cell Z ring assembly. *Mol. Microbiol.* **33**:33–40.
20. Harwood, C. R., and S. M. Cutting (ed.). 1990. *Molecular biological methods for Bacillus*. John Wiley and Sons, Chichester, England.
21. Hu, Z., A. Mukherjee, S. Pichoff, and J. Lutkenhaus. 1999. The MinC component of the division site selection system in *Escherichia coli* interacts with FtsZ to prevent polymerization. *Proc. Natl. Acad. Sci. USA* **96**:14819–14824.
22. Hutchison, C., and D. M. Glover (ed.). 1995. *Cell cycle control*. IRL Press, Oxford, England.
23. Ireton, K., D. Z. Rudner, K. J. Siranosian, and A. D. Grossman. 1993. Integration of multiple developmental signals in *Bacillus subtilis* through the Spo0A transcription factor. *Genes Dev.* **7**:283–294.
24. Jaacks, K. J., J. Healy, R. Losick, and A. D. Grossman. 1989. Identification and characterization of genes controlled by the sporulation-regulatory gene *spo0H* in *Bacillus subtilis*. *J. Bacteriol.* **171**:4121–4129.
25. Joseleau-Petit, D., D. Vinella, and R. D'Ari. 1999. Metabolic alarms and cell division in *Escherichia coli*. *J. Bacteriol.* **181**:9–14.
26. Katz, W., B. Weinstein, and F. Solomon. 1990. Regulation of tubulin levels and microtubule assembly in *Saccharomyces cerevisiae*: consequences of altered tubulin gene copy number. *Mol. Cell. Biol.* **10**:5286–5294.
27. Kelly, A. J., M. J. Sackett, N. Din, E. Quardokus, and Y. V. Brun. 1998. Cell cycle-dependent transcriptional and proteolytic regulation of FtsZ in *Caulobacter*. *Genes Dev.* **12**:880–893.
28. King, R. W., R. J. Deshaies, J. M. Peters, and M. W. Kirschner. 1996. How proteolysis drives the cell cycle. *Science* **274**:1652–1659.
29. Levin, P. A. 2002. Light microscopy techniques for bacterial cell biology, p. 115–132. *In* P. J. Sansonetti and A. Zychlinsky (ed.), *Molecular cellular microbiology*. Academic Press Ltd., London, England.
30. Levin, P. A., I. G. Kurtser, and A. D. Grossman. 1999. Identification and characterization of a negative regulator of FtsZ ring formation in *Bacillus subtilis*. *Proc. Natl. Acad. Sci. USA* **96**:9642–9647.
31. Levin, P. A., and R. Losick. 1996. Transcription factor Spo0A switches the



- localization of the cell division protein FtsZ from a medial to a bipolar pattern in *Bacillus subtilis*. *Genes Dev.* **10**:478–488.
32. **Levin, P. A., R. L. Schwartz, and A. D. Grossman.** 2001. Polymer stability plays an important role in the positional regulation of FtsZ. *J. Bacteriol.* **183**:5449–5452.
  33. **Lin, D. C.-H., P. A. Levin, and A. D. Grossman.** 1997. Bipolar localization of a chromosome partition protein in *Bacillus subtilis*. *Proc. Natl. Acad. Sci. USA* **94**:4721–4726.
  34. **Lu, C., J. Stricker, and H. P. Erickson.** 1998. FtsZ from *Escherichia coli*, *Azotobacter vinelandii*, and *Thermotoga maritima*—quantitation, GTP hydrolysis, and assembly. *Cell Motil. Cytoskelet.* **40**:71–86.
  35. **Lutkenhaus, J., and S. G. Addinall.** 1997. Bacterial cell division and the Z ring. *Annu. Rev. Biochem.* **66**:93–116.
  36. **Ma, X., D. W. Ehrhardt, and W. Margolin.** 1996. Colocalization of cell division proteins FtsZ and FtsA to cytoskeletal structures in living *Escherichia coli* cells by using green fluorescent protein. *Proc. Natl. Acad. Sci. USA* **93**:12998–13003.
  37. **Margolin, W.** 2001. Spatial regulation of cytokinesis in bacteria. *Curr. Opin. Microbiol.* **4**:647–652.
  38. **Perego, M., G. B. Spiegelman, and J. A. Hoch.** 1988. Structure of the gene for the transition state regulator *abrB*: regulator synthesis is controlled by the *spo0A* sporulation gene in *Bacillus subtilis*. *Mol. Microbiol.* **2**:689–699.
  39. **Pichoff, S., and J. Lutkenhaus.** 2002. Unique and overlapping roles for ZipA and FtsA in septal ring assembly in *Escherichia coli*. *EMBO J.* **21**:685–693.
  40. **Quardokus, E., N. Din, and Y. V. Brun.** 1996. Cell cycle regulation and cell-type specific localization of the FtsZ cell division initiation protein in *Caulobacter*. *Proc. Natl. Acad. Sci. USA* **93**:6314–6319.
  41. **Quardokus, E. M., and Y. V. Brun.** 2002. DNA replication initiation is required for mid-cell positioning of FtsZ rings in *Caulobacter crescentus*. *Mol. Microbiol.* **45**:605–616.
  42. **Quardokus, E. M., N. Din, and Y. V. Brun.** 2001. Cell cycle and positional constraints on FtsZ localization and the initiation of cell division in *Caulobacter crescentus*. *Mol. Microbiol.* **39**:949–959.
  43. **Quisel, J. D., W. F. Burkholder, and A. D. Grossman.** 2001. In vivo effects of sporulation kinases on mutant Spo0A proteins in *Bacillus subtilis*. *J. Bacteriol.* **183**:6573–6578.
  44. **Regamey, A., E. J. Harry, and R. G. Wake.** 2000. Mid-cell Z ring assembly in the absence of entry into the elongation phase of the round of replication in bacteria: co-ordinating chromosome replication with cell division. *Mol. Microbiol.* **38**:423–434.
  45. **Rothfield, L., S. Justice, and J. Garcia-Lara.** 1999. Bacterial cell division. *Annu. Rev. Genet.* **33**:423–448.
  46. **Rowland, S. L., V. L. Katis, S. R. Partridge, and R. G. Wake.** 1997. DivIB, FtsZ and cell division in *Bacillus subtilis*. *Mol. Microbiol.* **23**:295–302.
  47. **Sackett, M. J., A. J. Kelly, and Y. V. Brun.** 1998. Ordered expression of *ftsQ4* and *ftsZ* during the *Caulobacter crescentus* cell cycle. *Mol. Microbiol.* **28**:421–434.
  48. **Sambrook, J., E. F. Fritsch, and T. Maniatis.** 1989. *Molecular cloning: a laboratory manual*, 2nd ed. Cold Spring Harbor Laboratory Press, Cold Spring Harbor, N.Y.
  49. **Shapiro, L., and R. Losick.** 2000. Dynamic spatial regulation in the bacterial cell. *Cell* **100**:89–98.
  50. **Sun, Q., and W. Margolin.** 2001. Influence of the nucleoid on placement of FtsZ and MinE rings in *Escherichia coli*. *J. Bacteriol.* **183**:1413–1422.
  51. **Sun, Q., X. C. Yu, and W. Margolin.** 1998. Assembly of the FtsZ ring at the central division site in the absence of the chromosome. *Mol. Microbiol.* **29**:491–503.
  52. **Vicente, M., S. R. Kushner, T. Garrido, and M. Aldea.** 1991. The role of the 'gearbox' in the transcription of essential genes. *Mol. Microbiol.* **5**:2085–2091.
  53. **Wang, X., and J. Lutkenhaus.** 1993. The FtsZ protein of *Bacillus subtilis* is localized at the division site and has GTPase activity that is dependent upon FtsZ concentration. *Mol. Microbiol.* **9**:435–442.
  54. **Ward, J. E., Jr., and J. Lutkenhaus.** 1985. Overproduction of FtsZ induces minicell formation in *E. coli*. *Cell* **42**:941–949.
  55. **Weiss, D. S., J. C. Chen, J. M. Ghigo, D. Boyd, and J. Beckwith.** 1999. Localization of FtsI (PBP3) to the septal ring requires its membrane anchor, the Z ring, FtsA, FtsQ, and FtsL. *J. Bacteriol.* **181**:508–520.
  56. **Wu, L., and J. Errington.** 1994. *Bacillus subtilis* SpoIIIE protein required for DNA segregation during asymmetric cell division. *Science* **264**:572–575.
  57. **Wu, L. J., A. H. Franks, and R. G. Wake.** 1995. Replication through the terminus region of the *Bacillus subtilis* chromosome is not essential for the formation of a division septum that partitions the DNA. *J. Bacteriol.* **177**:5711–5715.
  58. **Yansura, D. G., and D. J. Henner.** 1984. Use of the *Escherichia coli* lac repressor and operator to control gene expression in *Bacillus subtilis*. *Proc. Natl. Acad. Sci. USA* **81**:439–443.